Agricultural operations planning in fields with multiple obstacle areas

Agricultural operations planning in fields with multiple obstacle areas

K.Zhou [a,*], A. Leck Jensen[a], C.G. Sorensen[a], P. Busato[b], D.D. Bochtis[a]

[a] Dept. of Engineering, Aarhus University, Blichers Allé 20, P.O. Box 50, 8830 Tjele, Denmark

[b] Dept. of Agricultural, Forest and Food Sciences (DISAFA), University of Turin, 10095 Grugliasco, Turin, Italy

Corresponding author. Tel.: +45 71474842.

Email address: kun.zhou@agrsci.dk.

Highlights

- Generation of feasible area coverage plan in fields with multiple obstacle areas.
- The optimization of the block sequence connection is formulated as a TSP problem.
- The developed model requires low computation time to compute the optimal block sequence.
- The error between the simulated and actual total travelled distance was 0.15% - 0.21%.

Abstract

When planning an agricultural field operation there are certain conditions where human planning can lead to low field efficiency, e.g. in the case of irregular field shapes and the presence of obstacles within the field area. The objective of this paper was to develop and implement a planning method for agricultural vehicles operating in fields inhabiting multiple obstacles. The developed approach consists of three stages. The first two stages regard the generation of the field geometrical representation where the field is split into sub-fields (blocks) and each sub-field is covered by parallel tracks, while the third stage regards the optimization of the block sequence aiming at minimizing the blocks connection travelled distance. The optimization problem was formulated as a TSP problem and it was solved implementing the ant colony algorithmic approach. To validate the developed model, two application experiments were designed. The results showed that the model could adequately predict the motion pattern of machinery operating in field with multiple obstacles. Errors of total distance travelled were 0.21% and 0.15% for the two experimental setups. Regarding the computation

time, the model required low computation times from 2.92 s in field with one obstacle to 11.51 s in field with two obstacles.

Keywords: route planning, agricultural vehicles, ant colony algorithm, traveling salesman problem.

1 Introduction

When planning an agricultural field operation there are certain field conditions where experience-based planning can lead to low machinery efficiency, for example the case of irregular field shapes and case of the presence of obstacles within the field area (Oksanen and Visala, 2007). So far, a significant amount of research has been carried out to solve the route planning problem in field operations. These advances include a number of methods for the geometrical field representation (de Bruin et al., 2009; Oksanen and Visala, 2009; Hofstee et al., 2009; Hameed et al., 2010) and a number of methods for route planning within a given field geometrical representation (Bochtis and Vougioukas, 2008; Bochtis and Sørensen, 2009; de Bruin et al., 2009; Bochtis et al., 2013, Scheuren et al., 2013).

In the case of fields with inhabited obstacles, in all developed methods the field is always decomposed into sub-fields (referred to as blocks). Due to the specific nature of field operations decomposition methods of the working space from the industrial robotics discipline area (Choset, 2001; Galeran and Carreras, 2013) cannot be directly applied. Oksanen and Visala (2007) developed a field decomposition method based on the trapezoidal decomposition for agricultural machines to cover the field. After decomposition, the trapezoids are merged into blocks under the requirements that the blocks have exactly match edges and the angles of ending edges is not too steep. Hofstee et al., (2009) developed a tool for splitting the field into single convex fields. Stoll (2003) introduced a method to divide the field into blocks based on the longest side of the field. Palmer (2003) presented a method of generating pre-determined tracks in fields with obstacles. Jin and Tang (2009) developed an exhaustive search algorithm for finding the optimal field decomposition and path directions for each subfield. However, in all of the above mentioned methods the optimum order to traverse the decomposed block was not derived. A first theoretical approach that provided the traversal sequence of the resulted blocks was presented in Hameed et al., (2013). The approach was based on the implementation

of genetic algorithms for the optimization of the visiting sequence of the different sub-field areas resulted by the presence of the obstacles. However, the computational requirements of the approach were exponential to the problem size (e.g. the number of obstacles in the field area) and the feasibility of the approach has not been tested in terms of their implementation on the real farming conditions.

The objective of this paper was to develop a planning method that generates a feasible plan for non-capacitated agricultural machines executing area coverage operations in fields inhabiting multiple obstacle areas. The method consists of three stages. The first two stages regard the generation of the field-work tracks and the division of the field into blocks, respectively, and the third stage regards the optimization of the sequence that the blocks are worked under the criterion of the minimization of the blocks connection distance. The problem of finding the optimal block traversal sequence was formulated as a travelling salesman problem (TSP) and it was solved by implementing the ant colony algorithmic approach

2 Methodology

2.1 Overview

The headland pattern is one of the most common field coverage patterns for agricultural machines, in which the field is divided into two parts, the headland area and field body area. The field body is the primary cropping area and it is covered with a sequence of straight or curved field-work tracks. The distance between two adjacent tracks is equal to the effective operating width of the agricultural machine. The headland area is laid out along the field border with the main purpose to enable the machines to turn between two sequential planned tracks. The order in which the agricultural machines operate in the two types of areas depends on the type of the operation; for example, the headland area is harvested before the field body, while the field body is seeded before the headland area. When a field has obstacles headlands are also laid out around the obstacles. The field body is split into a number of sub-fields (or blocks) around the obstacles, such that all blocks are free of obstacles.

The planning method involves the following three stages:

a) In the first stage, the field area and the in-field obstacle(s) are represented as a geometrical graph, This process includes the headland generation, the obstacle handling, and an initial generation of field-work tracks (ignoring the in-field obstacles until stage 2) (section 2.3).
b) In the second stage, the field body is decomposed into block areas and the previous generated field-work tracks are divided and clustered into these block areas (section 2.4).
c) In the third stage, the problem of the optimal traversal sequence of the blocks (in terms of area coverage planning) is derived (section 2.5).

The input parameters of the planning method include:

- The boundary of the field area and the boundaries of the in-field obstacles. All boundaries are expressed as a clock-wise ordered set of vertices.
- The number of the headland passes (h) for the main field and around each obstacle.
- The driving direction (θ). It determines the direction of the parallel fieldwork tracks that cover the field area.
- The operating width (w). This is the effective operating width of the implement and also represents the width of the field-work tracks.
- The threshold parameter (r), for the classification of the obstacle type (explained in section 2.2.2).

A graphical description of the proposed planning method is presented in the diagram in Fig. 1.

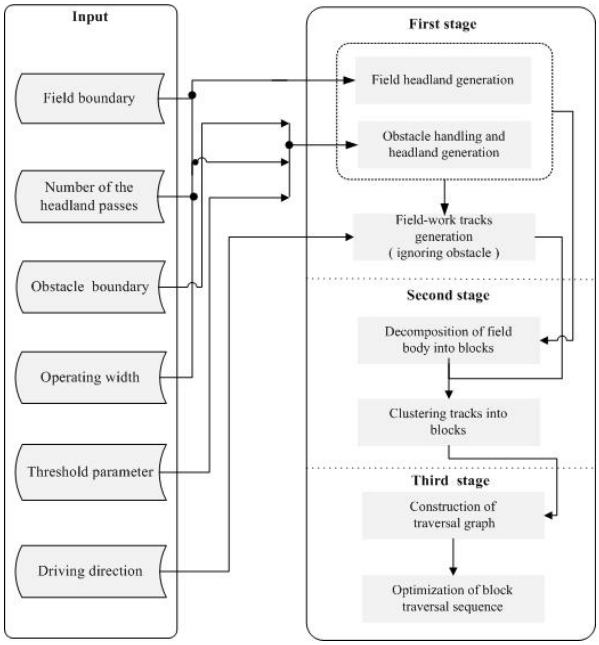

Fig. 1. The architecture of the proposed planning method.

2.2 First stage

2.2.1 Generation of field headland

The field headland area is obtained by offsetting the boundary inwardly by a width equal to the multiplication of the operating width, w times the number of headland passes, h. The distance from the field boundaries to the first headland pass is half of the operating width, $w/2$ while the distance between subsequent headland passes equals to the operating width, w. An inner boundary is created at distance $w/2$ from the last headland pass.

2.2.2 Categorizing of obstacles and generation of obstacles headlands

There are different types of obstacles in terms of their effect on the execution of a field operation. For example, certain physical obstacles due to their relatively small dimensions do not constitute an operational obstacle resulting in the generation of sub-fields (e.g. in Fig. 2a: Obstacle 5 is potentially such an obstacle). Other obstacles might exist that are close to the field boundary and the generation of sub-fields is not

104 required (e.g. obstacle 1 in Fig. 2). Finally, there are obstacles in close proximity that from the operational
105 point of view should be considered as one obstacle (e.g. obstacles 2 and 3 in Fig. 2).
106

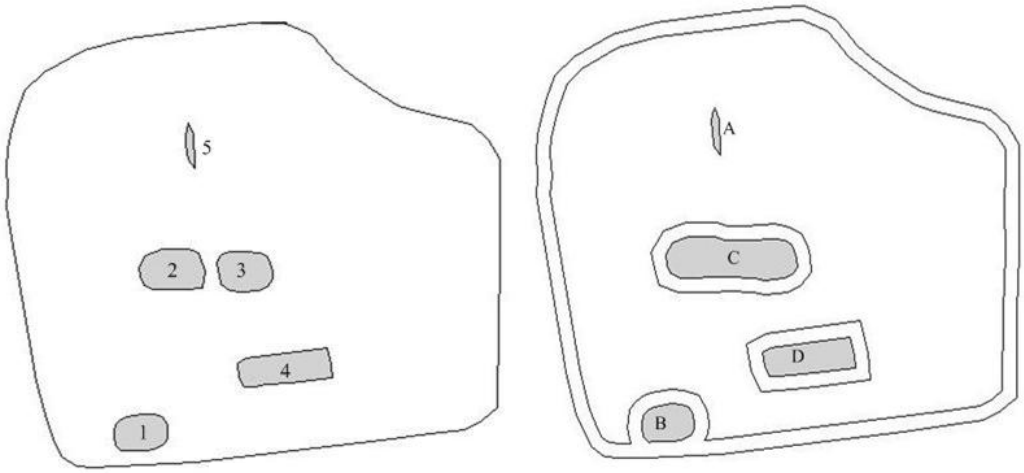

107 **(a)** **(b)**

108 **Fig. 2. Different obstacles configurations within a field area (a) and their classification (b).**

109 Four types of obstacles are defined:

110 Type A. An obstacle that due to size and configuration in relation to the driving direction does not affect the
111 coverage plan generation. In order to classify an obstacle as type A, the minimum boundary box of the
112 obstacle polygon is generated with one of its edges parallel to the driving direction. If the dimension, Δd of
113 the minimum bounding box that is perpendicular to the driving direction is less than the threshold parameter
114 r, this obstacle is considered as type A obstacle. Fig. 3a and Fig. 3b present how the driving direction θ
115 determines the classification of an obstacle as type A or not.

116 Type B. This type includes obstacles where their boundary intersects with the inner boundary of the field.
117 Type B obstacles are incorporated into the inner boundary of the field and the field headland is extended
118 around this obstacle.

119 Type C. This type includes obstacles where the minimum distance between another obstacles is less than the
120 operating width, w. In this case both obstacles are classified as of type C and a subroutine is used to find the
121 minimal bounding polygon to enclose these obstacles. For instance, assuming that the minimum distance

between the obstacle 2 and 3 in the Fig 2.a is less than the operating width, w, then the minimal bounding polygon (MBP) is gained by the sub-routine to represent the boundaries of these two obstacles as shown in Fig 2.b

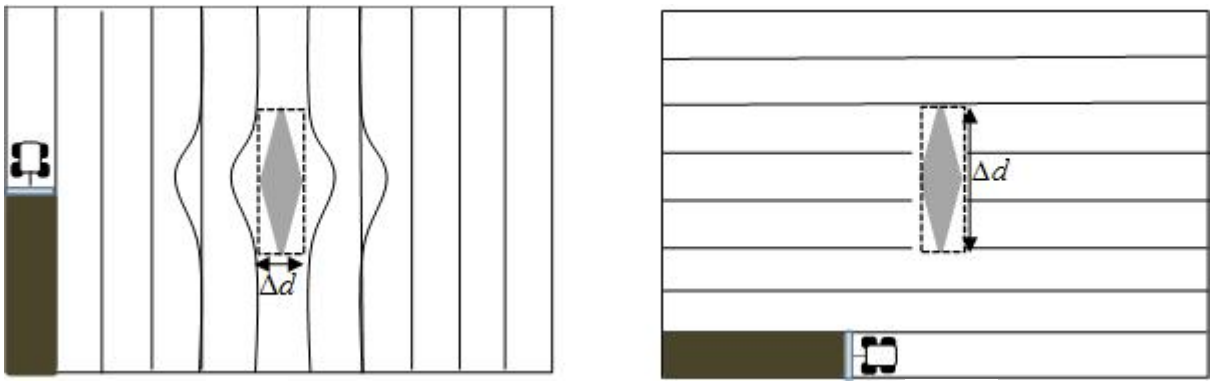

Fig. 3. The same obstacle can be classified as of type A (a) and as of type D (b) depending on the orientation of the obstacle as compared to the driving direction where $r = w$.

Type D. All remaining obstacles are considered as the Type D. Also the resulted new obstacles derived by the connection of two or more obstacles of type C are also classified as type D obstacles. Headland areas are generated only for the obstacles of type D. The method of generating obstacle headland is analogous to the method of field headland generation; however, the offset direction of the boundary is outward.

2.2.3 Generation of field-work tracks

Track generation concerns the process of generating parallel tracks to cover the field body. The minimum-perimeter bounding rectangle (MBR) of the inner field boundary is generated using the method of rotating calipers (Godfried, 1983). In the first step, depicted in the Fig. 4, the MBR is generated around the inner field boundary, and a reference line l parallel to θ is created intersecting one vertex on the MBR while let all other vertices of MBR located on the same half-plane determined by the line l. Let v be the vertex of the MBR with the longest perpendicular distance from l, and let v' be the projection of v on l. Then the number of the field-work tracks for a complete covering of the filed polygon area is given by $n = \lceil |vv'|/w \rceil$ (where $\lceil\ \rceil$ is the ceil function). The line segments to cover the entire MBR are generated

sequentially from the reference line l. The distance from l to the first line segment along the vv' equals to $w/2$, while the distance between the subsequent line segments along the vv' equals to w.

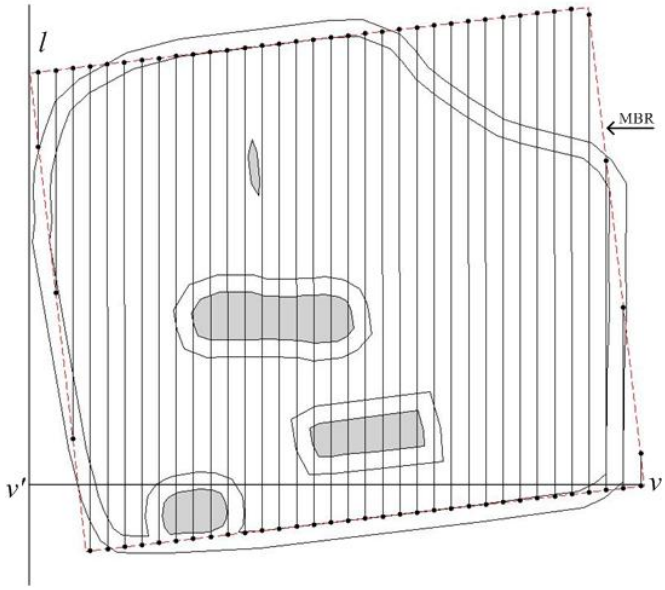

Fig. 4. The MBR of the field is covered by a set of straight lines that are parallel to the reference line *l*.

Let $T_0 = \{1,2,3...n\}$ denote the set of indices of these line segments, each of which intersects with the MBR in the form of two ending points on the MBR border. For each line segment $i \in T_0$, if it has n_i intersections with the inner field boundary it is subdivided into $n_i + 1$ new line segments. Each new line segment is checked if it is inside or outside the field body (disregarding the obstacles). If it is inside (the solid line segment in Fig. 5), the line segment is saved as a field-work track, otherwise it is discarded (the dash line segment in Fig. 5). In order to give each field-work track an index value, one of the two outmost tracks is arbitrary selected as the first track associating it with the index of value 1. Let $T = \{1,2,3...n'\}$ be the ordered set of the tracks.

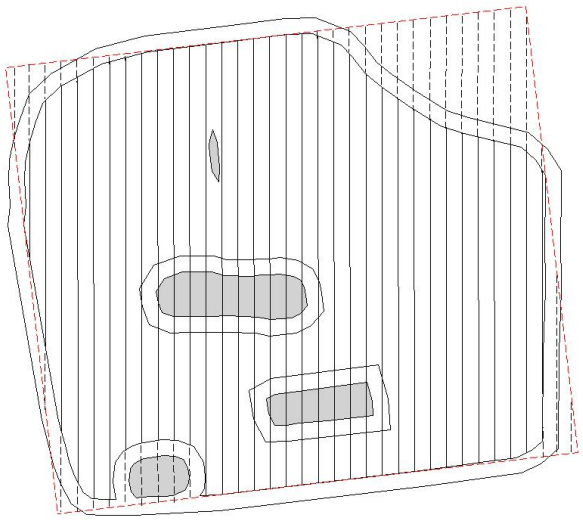

Fig. 5. Field body is covered by the field-work tracks (the solid lines)

2.3 Second stage

2.3.1 Decomposition of field body into blocks

In this step, the field body is decomposed into blocks, following the boustrophedon cellular decomposition method (Choset,1997). Specifically, a line, termed as a *slice,* parallel to the driving direction θ, sweeps through the inner field boundary from left to the right. Whenever the slice either meets a new obstacle (*in* event) or leaves an obstacle (*out* event) one or more preliminary blocks are formed behind the slice with block boundaries along the slice (See Fig. 6). When the decomposition is completed, an adjacency non-complete graph is built where each node of the graph represents a preliminary block and two nodes of the graph are connected only if there are common sections between the edges of the corresponding preliminary blocks (Fig. 7). The next step is to merge the generated preliminary block areas according to the adjacency graph. The merging requirement is that two connected blocks in the graph have a common edge. After the merging process, the generated block areas are indexed.

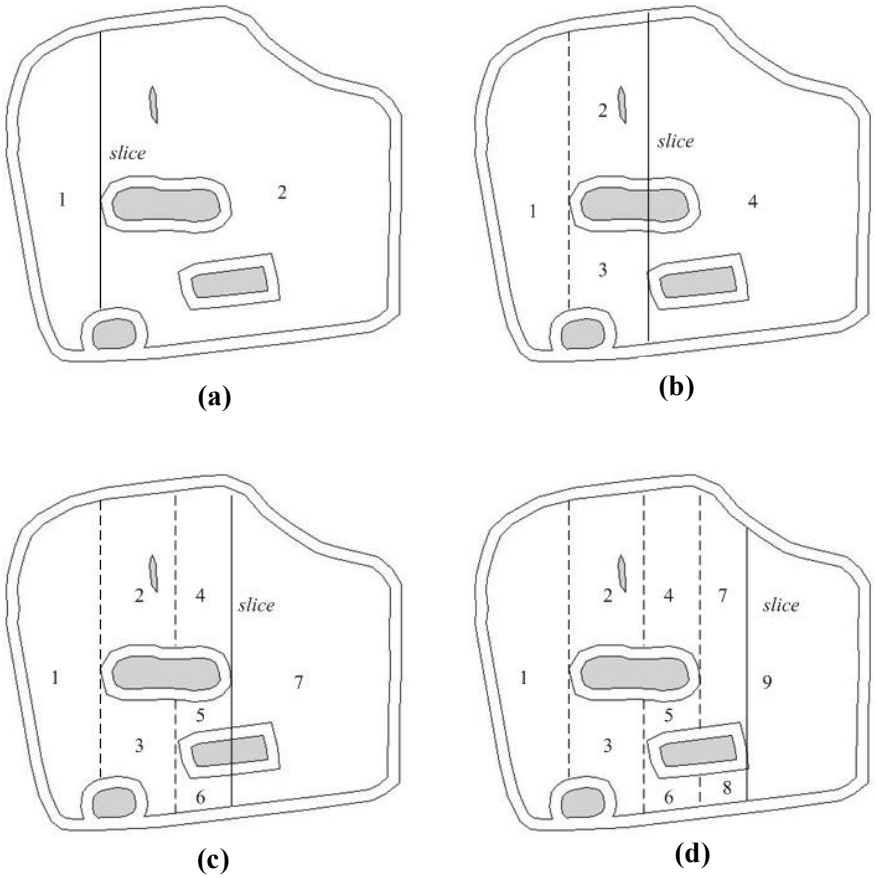

167

168 **Fig. 6. The sequential stages of the generation of the preliminary blocks**.

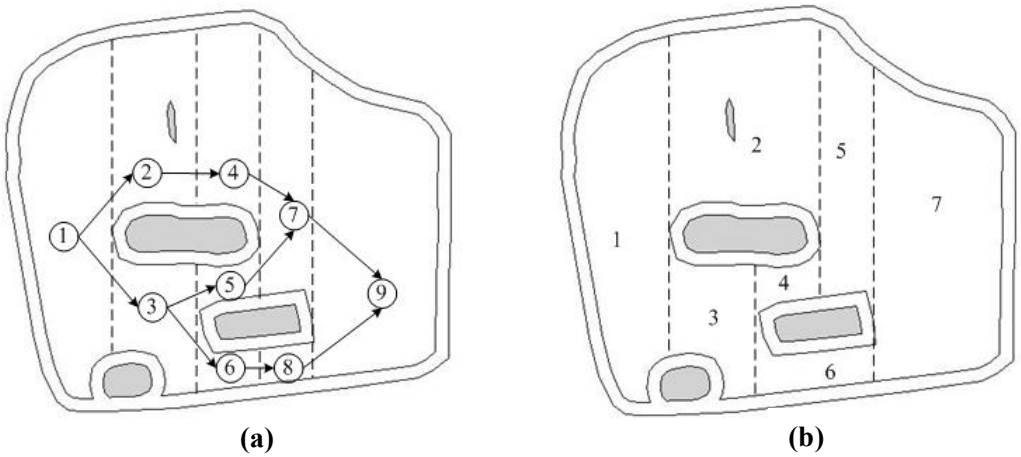

169

170 **Fig. 7. The adjacency graph of the preliminary blocks (a) and the final generated blocks.**

2.3.2 Clustering tracks into blocks

In the following, a method of dividing the generated tracks into segments and clustering the divided tracks into blocks areas is introduced.

Let $B = \{1,2,...,k\}$ be the generated block areas as described in section 2.3.1. The whole processing of clustering includes $\|T\|$ iterations. In each iteration, if a track $i \in T$ intersects with the boundary of a block area $j \in B$, it is subdivided into segments. The resulted segments are checked if they are located or not inside the area of block j. The segments located inside the block area are given the same index value with the index of the block. The set of the tracks in block $i \in B$ is denoted as $T_i, i \in B$.

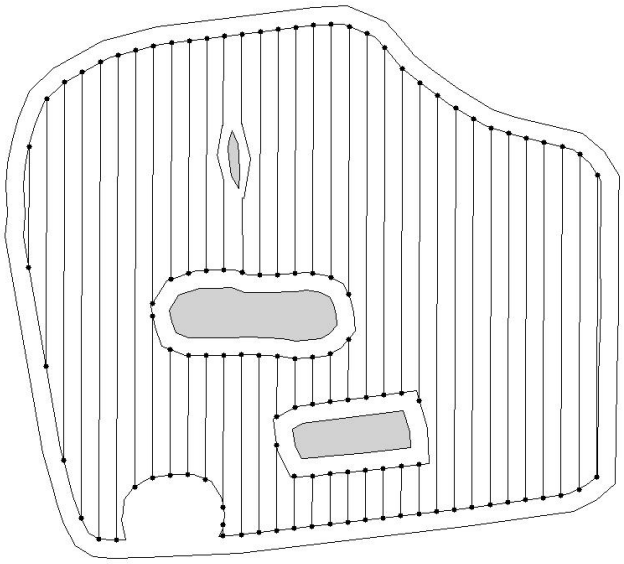

Fig. 8. Division and clustering of the initial tracks into the generated block areas.

2.4 Third stage

2.4.1 Construction of traversal graph

After the second stage the field has been divided into blocks and field-work tracks have been assigned to each block. Each block is a sub-field without obstacles, so the coverage of the corresponding area could be planned either using an optimized track sequence (e.g. *B-pattern*), or a conventional way of the continuous

track sequence can be used. On the presented work the latter case has been adopted and also the assumption that the work inside a block is always commenced in one of its two outmost tracks (the first or the last track of the block) has been considered. By making this assumption, each block can be represented by 4 entry/exit points: $N = \{n_{ij}, i \in B, j \in \{1,2,3,4\}\}$, where the nodes n_{i1} and n_{i2} are end points of the first track and n_{i3}, n_{i4} are end points of the last track of block j. For a given block the exit point is determined by the entry point and the parity of the number of the tracks of the block. For example, considering block 1 in Fig. 9 which has an even number of tracks, for the case of the continuous pattern if the operation commences at the end of the track corresponding to node n_{12}, then the operation will be completed at the end of the last track corresponding to node n_{14}.

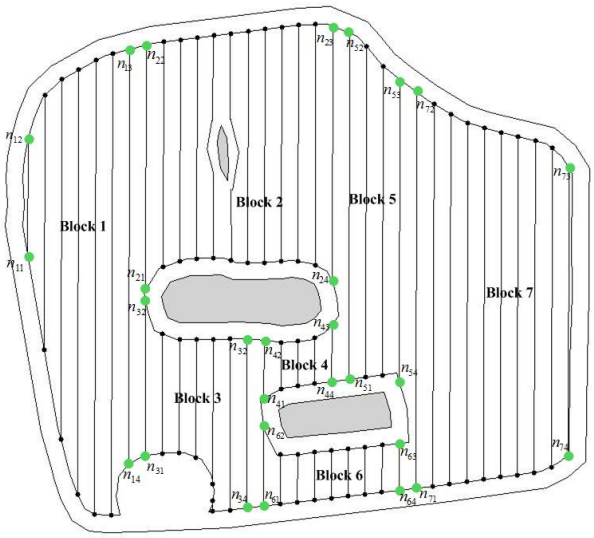

Fig. 9. An example of a simple devised field with an obstacle, resulting in 4 blocks.

The problem of the block sequencing is equivalent with the problem of traversing the undirected, weighted graph $G = \{N, E\}$, where N is the set of graph nodes as defined previously, and E is the set of edges, consisting of paths between any entry/exit points. Each edge $E_{n_{ix}n_{jy}}, n_{ix} \neq n_{jy}$ is associated with a weight $c_{n_{ix}n_{jy}}, n_{ix} \neq n_{jy}$ which corresponds to the transit cost from node n_{ix} to node n_{jy}. Although G can be considered as a complete graph, some potential connections between nodes within a block are not allowed while others

have to be enforced. For each block the function $e_i = (-1)^{\mathrm{mod}(|T_i|,2)}$ is defined and its value (1 or -1) depends on the parity of the number of the tracks in the block. By using this function the cost for the connection between nodes belonging to the same block is given by: $c_{n_{i1}n_{i2}} = c_{n_{i3}n_{i4}} = 0$, $c_{n_{i2},n_{i3}} = c_{n_{i1}n_{i4}} = L^{-e_i}$, and $c_{n_{i2}n_{i4}} = c_{n_{i1}n_{i3}} = L^{e_i}$, where L is a (relatively) very large positive number.

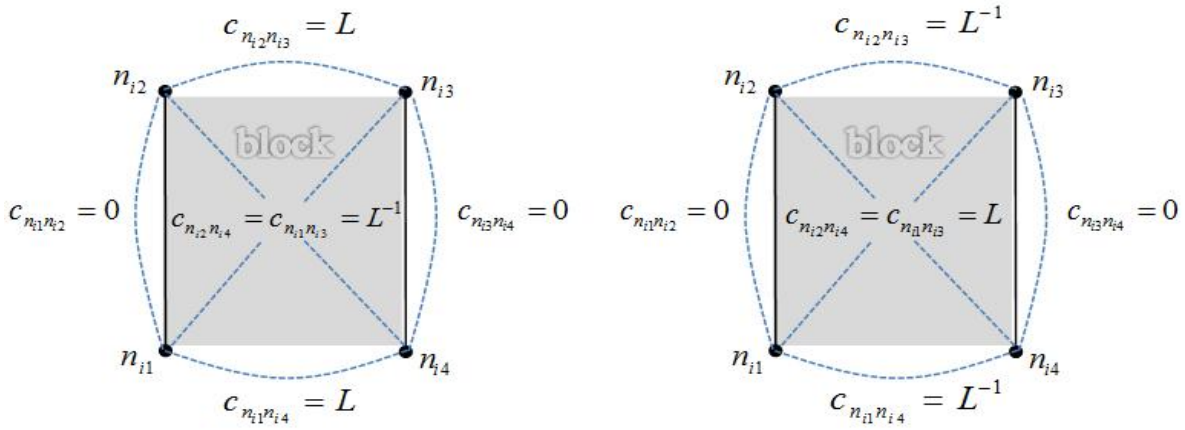

Fig. 10. Internal cost assignment for blocks with odd (a) or even number of tracks (b)

In order to avoid connections between blocks that in the physical operation will result to the situation where machine travels on a part of the field main area in order to move from one block to the other, both of the blocks must have nodes that are located either on the inner boundary of the field or in the outer boundary of the same obstacle in order to allow a connection between two blocks,.

For each pair of nodes of graph *G* a binary function $s(n_{ix}, n_{jy})$ is defined which returns the value 1 if n_{ix} and n_{jy} are both located either on the inner boundary of the field or on the outer boundary of an obstacle, and value 0 otherwise. If $s(n_{ix}, n_{jy}) = 1$ the cost for the connection of n_{ix} and n_{jy} is the actual shortest distance along the headland pass of the field or the obstacle. In contrast, a relatively large number, L, is assigned to the cost $c_{n_{ix}n_{jy}}$ when $s(n_{ix}, n_{jy}) = 0$.

2.4.2 Optimization of block traversal sequence

Since the problem graph has been considered as a complete graph, the problem of finding the shortest path for visiting all blocks is equivalent to finding the Hamiltonian path through the constructed graph *G*, which is equivalent to the travelling salesman problem (TSP) (Hahsler, 2007). The TSP is a well-known combinatorial optimization problem, which is non-deterministic Polynomial-time hard (NP-hard) problem (Garey and Johnson, 1979) and various algorithmic approaches have been developed based on exact solution approaches (e.g. branch-and– bound, and branch-and-cut, etc.) and approximate approaches (e.g. tabu search genetic algorithm and ant colony algorithm, etc.) (Glover and Kochenberger, 2002). For the particular problem presented here, any of the developed TSP solving methods can be implemented, in principle, since the size of the computational problem is relatively small. This is due the fact that the number of obstacles in an agricultural field is limited because of operational considerations.

Among the different solving methods the ant colony (ACO) algorithm has been selected. ACO is a mathematical model based on ants behavior in finding the shortest route between ant colonies and food sources. The principle is based on the fact that every ant deposits pheromone on the traveled path. For a detailed description of the method refer to Dorigo (1996). In the presented problem, the cost of the connection of two nodes, $c_{n_{ix}n_{jy}}, i, j \in B, x, y \in \{1,2,3,4\}$, is connected with the so-called heuristic value for moving between the two nodes in the ACO notion. Beyond the cost matrix, the parameters that have to be quantified in the ACO are parameter ρ which represents the evaporation rate of the pheromone, and parameters α, and β which are adjustable parameters to weight the importance of the pheromone.

3 Results and discussion

3.1 Feasibility of the method

To evaluate the feasibility of the plan generated by the method, the simulated output for two field operations were compared with the actual planned and performed operations by the farmer in two fields. The first field

included one obstacle and has an area of 16.16 ha (Fig. 11a). The second field included two obstacles and has an area of 24.25 ha (Fig. 11b). The specific operations involved potato seedbed forming and harrowing. The trajectory of the tractor was recorded using an AgGPS 162 Smart Antenna DGPS receiver (Trimble, GA, USA). Its accuracy is ± 20.3-30.5 cm pass-to-pass. In order to provide the model with the accurate data on field geometry, the vertices along the field edges were measured by tracking the field boundaries with the same GPS receiver. The Douglas- Peucker line simplification algorithm (Douglas and Peucker, 1973) was applied to process the GPS coordinates of the field geometry.

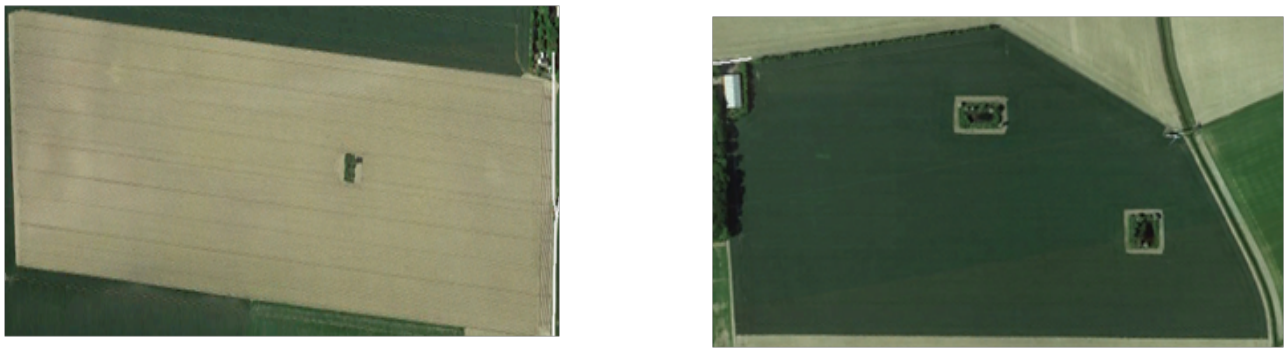

(a) **(b)**

Fig. 11. The selected experimental fields: field A (a) and field B (b).

3.1.1 Field A

3.1.1.1 Experimental operation

For the operation in field A, an AB line was set and set for the navigation system by driving the tractor along the longest edge of the field from one headland to the opposite headland. The operating width was 4.95 m while the turning radius of the tractor was 6 m. The coverage of the field was performed following the continuous fieldwork pattern. Based on the analysis of the GPS recordings (Fig. 12), the measured effective working distance was 32,823 m, the measured non-working headland turn distance was 1,720.2 m and the connection distance of blocks was 112.3 m. The average effective operating speed was 1.2 m/s, while the average turning speed was 0.85 m/s.

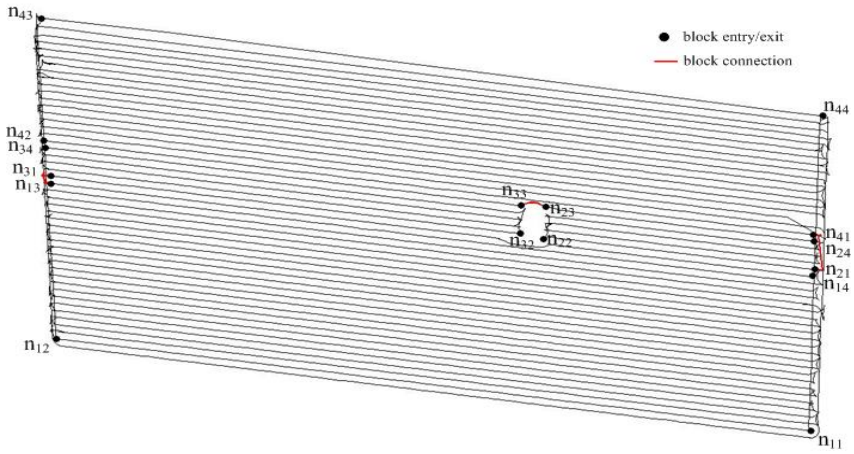

Fig. 12. The GPS recordings of operation in field A

3.1.1.2 Simulated operation

The operating width, the turning radius and the driving direction for the simulated operation were the same as in the experimental one (4.95 m and 6 m and 143.5° respectively), resulting in 49 tracks and 4 blocks. The headland passes number was also selected to be 2 as in the actual operation.

For finding the shortest connection distance of blocks, the total number of ants, m, was set to 16, while ρ, α and β were set to 0.5, 1, and 5, respectively； these values were experimentally found to provide the best solutions by Colorni (1992) .The number of iteration was 200. Ten runs were performed with an average computational time of 2.92 s.

The optimal sequence of the blocks and the corresponding entry and exit nodes was: {[n_{11} n_{12} n_{14} n_{13}] -> [n_{31} n_{32} n_{34} n_{33}] -> [n_{23} n_{24} n_{22} n_{21}] -> [n_{41} n_{42} n_{43} n_{44}]}.The estimated total effective distance, including the infield working distance and the working distance in the headlands, during the whole operation was 32,791 m. The estimated non-working headland turn distance was 1,682.5 m. The connection distance of the blocks was 106.9 m.

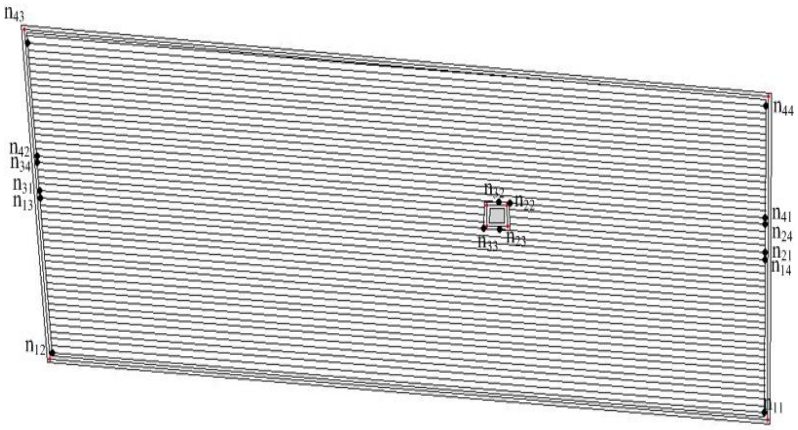

273

274 **Fig. 13. The generated plan for field A**

275 **3.1.2 Field B**

276 *3.1.2.1 Experimental operation*

277 In the operation in field B the operating width was 12 m and the turning radius of the tractor was 6.5 m.
278 Based on the analysis of the GPS recording (Fig. 14), the measured effective working distance was 19,643
279 m, the measured non-working headland turn distance was 1,370 m and the connection distance of blocks was
280 450.4 m. The average effective operating speed was 1.5 m/s, while the average turning speed was 0.9 m/s.

281

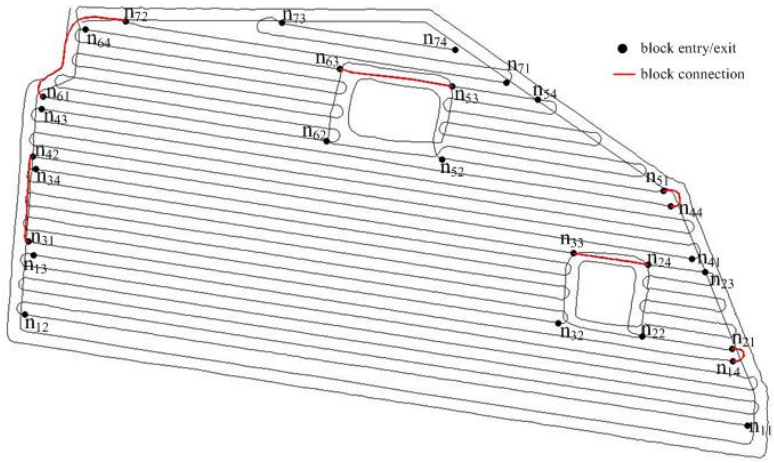

282

283 **Fig. 14. The GPS recordings of operation in field B**

3.1.2.2 *Simulated operation*

The operating width, the turning radius and the driving direction for the operation were the same as in the actual operation (12 m and 6.5 m and 172.5° respectively), resulting in 44 tracks and 7 blocks. The headland passes number was set to 2 as in the actual operation.

For finding the shortest connection distance of blocks, parameters of the ACO algorithm were set as: $\rho = 0.5, \alpha = 1$, and $\beta = 5$, and the number of iteration was 200. The number of the ants used was 28 which equals to the number of the nodes presenting the entry and exit points of blocks. Ten runs were performed with an average computational time of 11.51 s.

The optimal sequence of the blocks and the corresponding entry and exit nodes was:

{[n_{11} n_{12} n_{13} n_{14}] - > [n_{21} n_{22} n_{24} n_{23}] -> [n_{33} n_{34} n_{32} n_{31}] -> [n_{42} n_{41} n_{43} n_{44}] -> [n_{51} n_{52} n_{54} n_{53}]-> [n_{63} n_{64} n_{62} n_{61}]->[n_{72} n_{71} n_{73} n_{74}]}.The estimated total effective distance, including the infield working distance and the working distance in the headlands, during the whole operation was 19,634 m. The estimated non-working headland turnings distance was 1,350.5 m. The connection distance of the blocks was 445.3 m.

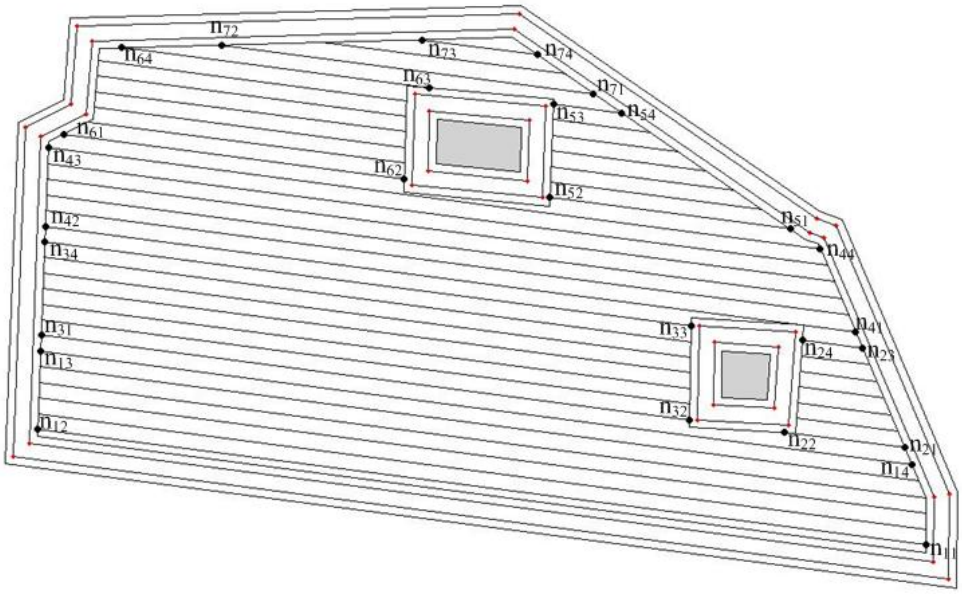

Fig. 15. The generated plan for field B

3.2 Comparison between simulated and experimental results

The comparison between the experimentally performed and planned operation and the simulated operation shows that the developed method can simulate the field operation with sufficient accuracy. As shown in Table 1, the prediction error in terms of total travelled distance was 0.21% for field operation A and 0.15% for field operation B. The relatively small errors between the measured and the predicted values of the operational time elements are mainly arisen from two reasons. First, due to the actual conditions of the field surface and the positioning error, the vehicle cannot exactly follow the planned parallel tracks. In addition, the GPS guidance system only navigate on the in-field parallel tracks while the turnings in the headland areas of the field and the obstacles were manually executed and was depended on the driver's abilities.

Table 1- Comparison between the data from the experimental and the simulated operations

	Operation A			Operation B		
	Simulated (m)	Measured (m)	Error (%)	Simulated (m)	Measured (m)	Error (%)
Total effective distance	32,791	32,823	0.10	19,634	19,643	0.045
Non-working distance	1,682.5	1,720.2	2.23	1,350.5	1,370	1.4
Connection distance of blocks	106.9	112.3	5.05	445.3	450.4	1.14
Total travelled distance	34,580.4	34,655.5	0.21	21,429.8	21,463.4	0.15

To test the performance of the ACO algorithm for the solution of the optimization part of the method, an exhaustive algorithm was used to obtain the optimal block sequence examining all the combinations of the blocks connections in both cases of field A and field B. The exhaustive algorithm provided the same solutions as the ACO for both cases. For the field A, the exhaustive algorithm provided the optimal block sequence in 0.58 s while the ACO algorithm provided the same solution in 2.92 s. However, as the number of in-field obstacle increased to two in case of field B, the computational time of the exhaustive algorithm increased to 560.8 s while the computational time for the ACO algorithm was 9.98 s. This was expected

since the computational steps and consequently the computational time of the exhaustive enumeration algorithm increases exponentially with the size of the problem making it unfeasible for medium to large scale problems (e.g. up to 3-4 blocks).

3.3 Simulated test cases

In order to demonstrate how the developed method can handle more complicated cases, three fields, including 3, 4, and 5 obstacles, respectively, were selected. The parameters regarding the input and output are shown in the Table 2 while the solutions are presented in Fig 16. As expected, the computational time was increased as the number of obstacles was increased. However, it has to be noted that, regarding the number of the iterations, as the number of the obstacle increases, more iterations are needed to guarantee than the best solution can be obtained.

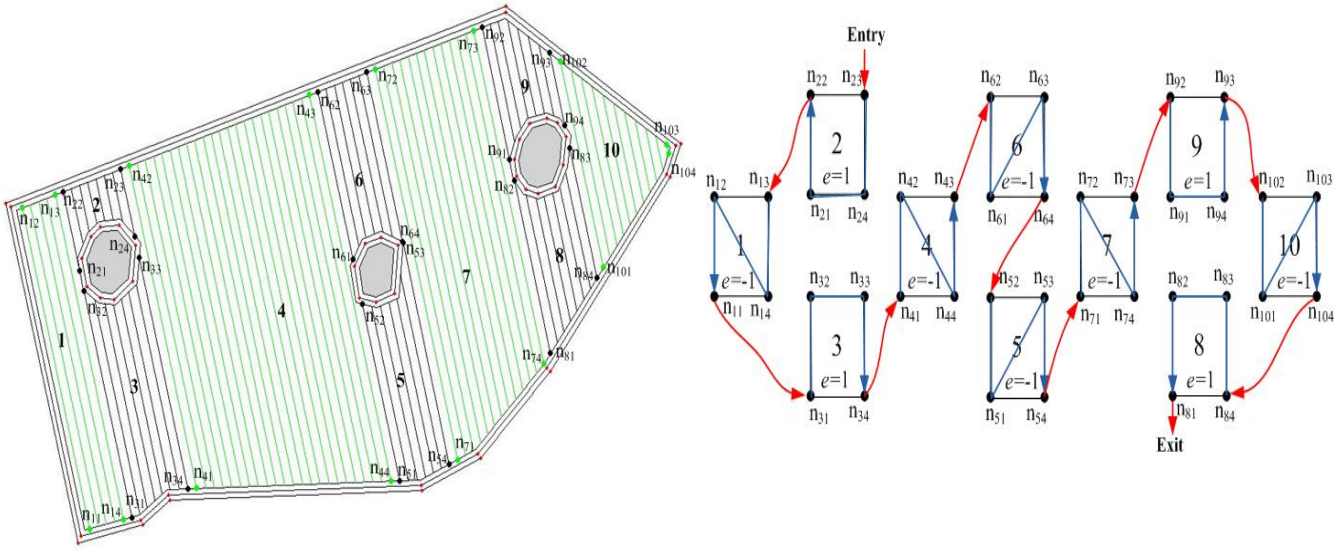

(a)

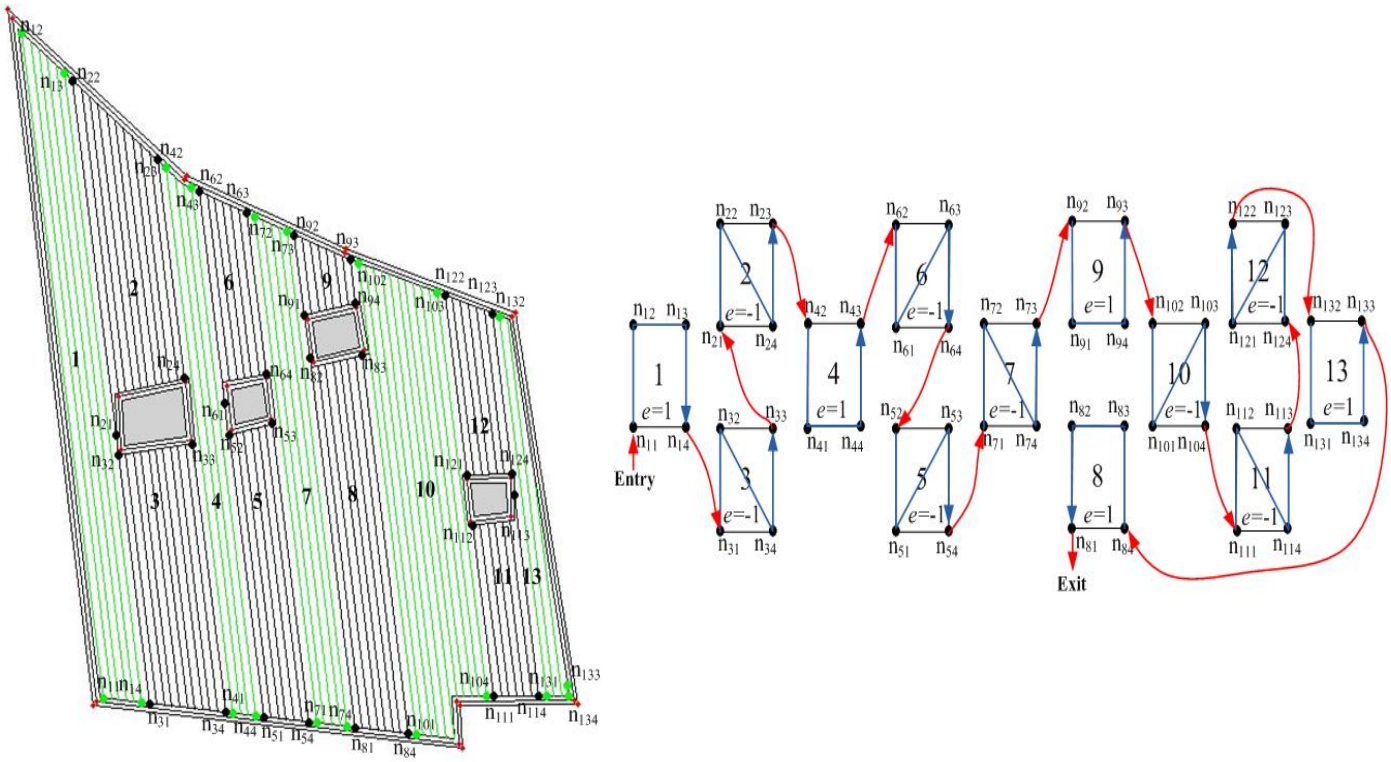

328

329 **(b)**

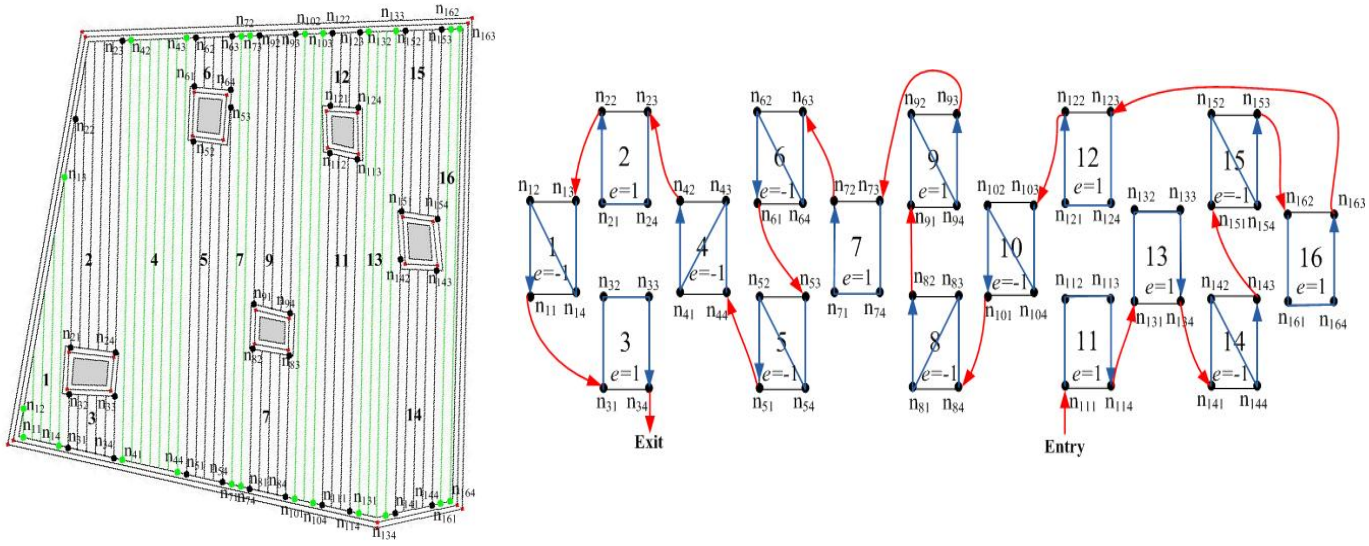

330

331 **(c)**

332 **Fig.15. The resulted solution of the method for the test cases regarding fields with (a) 3 obstacles, (b) 4**

333 **obstacles, and (c) 5 obstacles**

334 **Table 2. Parameters and results from the three simulated test cases**

Field	(a)				(b)				(c)			
Area(ha)	20.21				56.54				4.81			
Number of obstacles	3				4				5			
Driving angle(°)	105				108.2				31.8			
Operating width (m)	9				12				15			
Minimum turning radius (m)	6				6				6			
Number of headland passes	1				1				1			
ρ	0.5				0.5				0.5			
α	1				1				1			
β	5				5				5			
Iterations	50	100	200	400	100	200	400	600	100	200	400	600
Average processing time (s)	15.2	27.5	55.1	109.3	69.4	118.3	233.7	400.4	123.3	235.5	465.8	697.7
Blocks connection distance (m)	371.5	371.5	371.5	371.5	765.1	765.1	765.1	765.1	856.4	856.4	856.4	856.4
Total effective working distance (m)	21,823				46,020				31,680			
Non-working distance (m)	2,973.9				1,790.7				1,573.2			

335

336 # 4 Conclusions

337 In this paper, a planning method for simulating field operations in fields with multiple obstacle areas was
338 presented. The method implies that the field is divided into blocks when considering the in-field obstacle(s)
339 and the optimal block traversal sequence was formulated as a TSP problem which is solved by applying the
340 ACO algorithmic approach.

341 The validation of the method showed that it can simulate field operations with sufficient accuracy. Based on
342 two experimental set-ups, the errors in the prediction of total travelled distance were 0.15% and 0.21%,

343 respectively. Furthermore, the optimization part of the method was validated by compared the ACO
344 algorithm solutions with an exhaustive enumeration algorithm for the small-sized problems included in the
345 two previously mentioned cases.

346 It was also demonstrated that the method can provide feasible solutions for more complicated field
347 operational environments in terms of the number of obstacles included in the field area. Even in the cases of
348 conditions seldom experienced in practice, e.g. involving 5 obstacles, the computational time of the method
349 was less than 700 s.

350 The developed method can be used as part of a decision support system providing feasible field operation
351 solutions in testing different driving directions, operating widths, machine turning radius etc. Furthermore,
352 the method can be incorporated in navigation-aiding systems for agricultural machinery since currently such
353 systems cannot provide a complete route for covering fields that include obstacles.

354 # 5 References

355 Bochtis, D.D., Sørensen, C.G., 2009. The Vehicle Routing Problem in Field Logistics Part I. Biosystems
356 Engineering 104(4), 447 - 457.

357 Bochtis, D.D., Sørensen, C.G., 2010. The vehicle routing problem in field logistics: Part II. Biosystems
358 Engineering 105(2), 180 - 188.

359 Bochtis, D.D., Vougioukas, S.G., 2008. Minimising the non-working distance travelled by machines
360 operating in a headland field pattern. Biosystems Engineering, 101(1), 1 - 12.

361 Bochtis, D.D., Sørensen, C.G., Busato, P., Berruto, R., 2013. Benefits from optimal route planning based on
362 B-patterns. Biosystems Engineering 115 (4), 389 - 395.

363 Choset, H., 2001. Coverage for robotics - a survey of recent results. Annals of Mathematics and Artificial
364 Intelligence 31, 113 - 126.

365 Choset, H., Pignon, P., 1997. Coverage Path Planning: The Boustrophedon Decomposition. International
366 Conference on Field and Service Robotics, 1997.

367 Colorni, A., Dorigo, M., & Maniezzo, V., 1992. An Investigation of some Properties of an "Ant Algorithm".
368 PPSN 92, 509-520.

369 Dorigo, M., Gambardella, L. M., 1997. Ant colony system: A cooperative learning approach to the traveling
370 salesman problem. Evolutionary Computation, IEEE Transactions on, 1(1), 53 - 66.

371 Douglas, D., Peucker, T., 1973. Algorithms for the reduction of the number of points required to represent a
372 digitized line or its caricature, The Canadian Cartographer 10(2), 112 -122.

373 de Bruin, S., Lerink, P., Klompe, A., Van derWal, D., Heijting, S., 2009. Spatial optimisation of cropped
374 swaths and field margins using GIS. Computers and Electronics in Agriculture 68(2), 185 -190.

375 Galceran, E., Carreras, M., 2013. A survey on coverage path planning for roborics. Robotics and
376 Autonomous Systems 61(12), 1258 - 1276.

377 Garey, M., Johnson, D., 1979. Computers and Intractability: a Guide to the Theory of NP-Completeness

378 Freeman, San Francisco, CA, USA .

379 Glover, F., Kochenberger, G., 2002. Handbook of Metaheuristics. Kluwer Academic Publishers, Norwell,
380 MA, USA.

381 Toussaint G.T., 1983. Solving geometric problems with the rotating calipers. In: Proceedings of
382 MELECON,83.

383 Hameed, I.A., Bochtis, D.D., Sørensen, C.G, Nørremark, M.A ., 2010. Automated generation of guidance
384 lines for operational field planning. Biosystems Engineering 107 (4), 294 - 306.

385 Hofstee, J.W., Spätjens L.E.E.M., IJken.H., 2009. Optimal path planning for field operations. Proceedings
386 of the 7th European Conference on Precision Agriculture. Wageningen Academic Publishers, The
387 Netherlands, 511-519.

388 Hameed, I.A., Bochtis, D.D., Sørensen, C.G., 2013. An optimized field coverage planning approach for
389 navigation of agricultural robots in fields involving obstacle areas. International Journal of
390 Advanced Robotic Systems 10, 1 - 9.

391 Hahsler, M., Hornik, K., 2007. TSP - Infrastructure for the Traveling Salesperson Problem. Journal of
392 Statistical Software 23(2), 1 - 21.

393 Jian, J, Lie, T, 2010. Optimal coverage path planning for arable farming on 2D surfaces. Transactions of the
394 ASABE, 53 (1) , 283 -295.

395 Oksanen, T. and Visala, A., 2007. Path planning algorithms for agricultural machines. Agricultural
396 Engineering International, The CIGR Journal, Volume IX.

397 Oksanen, T. and Visala, A., 2009. Coverage path planning algorithms for agricultural field machines.
398 Journal of Field Robotics 26 (8), 651 - 668.

399 Palmer, R. J., Wild, D., Runtz K., 2003. Improving the efficiency of field operations. Biosystems
400 Engineering 84(3) 283 - 288.

401 Stoll, A., 2003. Automatic operation planning for GPS-guided machinery. In: J Stafford and A Werner
402 (Eds.), Proceedings of the 4th European Conference on Precision agriculture. A. Wageningen
403 Academic Publishers, The Netherlands. 657 - 644.